

INSTRUMENTS AND METHODS OF INVESTIGATION

PACS numbers: 73.50.Jt, **85.75. – d**, 85.80.Lp

Galvanomagnetic and thermomagnetic phenomena in thin metal CoPt films

Yu M Kuznetsov, M V Dorokhin, A V Zdoroveyshchev,
A V Kudrin, P B Demina, D A Zdoroveyshchev

DOI: https://doi.org/10.3367/UFNe.2021.11.039108

Contents

Abstract. The paper presents the results of a study of the magnetic field dependences of the Hall and Nernst–Ettingshausen coefficients in a wide temperature range of 10–370 K in a thin ferromagnetic CoPt film formed on a semi-insulating gallium arsenide substrate by electron beam evaporation in a vacuum. The presence of the dominant contribution of the anomalous component of the effects in the entire investigated temperature range is shown. The experimentally obtained temperature dependences of the amplitude of the effects are presented, and they are compared with the theoretical model.

Keywords: Hall effect, Nernst–Ettingshausen effect, spin-dependent scattering, scattering factor, spintronics

1. Introduction

The Nernst–Ettingshausen thermomagnetic effect is well known in the literature as a method for determining electronic properties of semiconductor and metallic materials, complementing Hall effect measurements [1]. In particular, the Hall effect measurements allow calculating the concentration and mobility of charge carriers to the Hall factor A_r, a constant depending on the scattering mechanism in a particular material [2]. Most often, the value of the Hall factor is set to one, which introduces an error to the calculated values of the Hall parameters (since the Hall factor can take values in the interval from 0 to 1.93). Measurements of the Nernst–Ettingshausen effect are similar to those of the Hall effect, but, instead of a longitudinal potential difference in the material, a temperature gradient is set and, as in the Hall effect, the transverse voltage arising in an external magnetic field perpendicular to the plane of current flow is measured. The obtained magnetic field dependences of the Nernst–Ettingshausen voltage provide additional equations needed to calculate the Hall factor and, therefore, allow calculating the concentration and mobility of free charge carriers with higher accuracy [3]. Note that for semiconductor structures it is most often necessary to determine the concentration of charge carriers with an accuracy of an order of magnitude. For such an estimate, the study of the Hall effect is sufficient, which is why the technique of measuring thermomagnetic effects is not widely used.

An interesting variant of the Nernst–Ettingshausen effect is an anomalous effect consisting of a distortion of the linear magnetic field dependence of the arising transverse thermomagnetic voltage. Such a phenomenon is observed in paramagnetic and ferromagnetic materials and is related to specific features of the spin-dependent scattering of free charge carriers by magnetic centers [4–6]. In the case of a structure being in a ferromagnetic state, the magnetic field dependence of the Nernst–Ettingshausen voltage can take the form of a hysteresis loop. In Refs [7, 8], it is shown that, by measuring the anomalous Nernst–Ettingshausen effect and calculating the appropriate coefficients, it is possible to make conclusions on both the character of spin-orbital coupling and the ferromagnetic electronic structure. Thus, the above measurements can be used to analyze new magnetic materials.

From a practical point of view, it is important to note that the Nernst–Ettingshausen voltage can be additive with the thermoelectric effect, thus contributing to the Seebeck coefficient. The physics of thermoelectric phenomena is a large field of scientific and practical activity, the purpose of which is to create autonomous energy converters that use

Yu M Kuznetsov [1,2,a], **M V Dorokhin** [2,b], **A V Zdoroveyshchev** [2,c], **A V Kudrin** [1,2,d], **P B Demina** [2,e], **D A Zdoroveyshchev** [1,2]
[1] Lobachevsky State University,
prosp. Gagarina 23, 603920 Nizhny Novgorod, Russian Federation
[2] Research Institute for Physics
and Technology of Lobachevsky State University,
prosp. Gagarina 23, 603920 Nizhny Novgorod, Russian Federation
E-mail: [a] yurakz94@list.ru, [b] dorokhin@nifti.unn.ru,
[c] zdorovei@nifti.unn.ru, [d] kudrin@nifti.unn.ru,
[e] demina@phys.unn.ru

Received 23 August 2021, revised 19 November 2021
Uspekhi Fizicheskikh Nauk **193** (3) 331 – 339 (2023)
Translated by V L Derbov

waste heat from technological, industrial, or domestic processes [9–11]. The energy conversion efficiency (thermoelectric quality factor) depends on the characteristics of the material used and is described by the dimensionless quantity $ZT = \alpha^2 T/(\rho\lambda)$, where α is the Seebeck coefficient, characterizing the dependence of the arising thermoelectric effect on the temperature gradient value, T is the mean temperature, ρ is the specific resistance, and λ is the heat conduction coefficient.

Metal-based thermoelectric materials, as a rule, are not considered in the physics and technology of thermoelectrics because of their extremely low Seebeck coefficient. The Nernst–Ettingshausen voltage added to the thermoelectromotive force (thermal EMF) allows a substantial increase in the coefficient α and, therefore, an increase in the value of ZT to a competitive level [12]. Thus, Refs [13, 14] experimentally show an increase in the efficiency of heat conversion by using the thermomagnetic Nernst–Ettingshausen effect in layers of CoFe and MnSb, respectively. The authors of Ref. [15] report an increase in the thermoelectric efficiency coefficient to $ZT = 0.5$ in $Li_{0.9}Mo_6O_{17}$ metal because of the Nernst–Ettingshausen voltage arising in an external magnetic field with an induction of 90,000 Oe. Of great interest is the study of the thermomagnetic effect in thin films with high magnetic anisotropy. For example, Ref. [16] studied the anomalous Nernst–Ettingshausen effect in $L1_0-FePt$ films. Reference [17] proposes a method of significant thermomagnetic effect enhancement in such films by creating a multilayer structure, whose layers possess the anomalous Nernst–Ettingshausen effect of different signs. The authors of [17] presented data on the enhancement of the effect in the $L1_0-FePt/MnGa$ structure as compared to the $L1_0-FePt$ structure. Similar studies were performed in Ref. [7], where the anomalous Nernst–Ettingshausen effect in Fe_3O_4 films was investigated. Important practical advantages of ferromagnetic thermoelectric generators can be high radiation resistance and temperature stability compared to the most commonly used semiconductor thermoelectrics. In this regard, of particular interest are complex ferromagnetic alloys with anomalously high Nernst–Ettingshausen voltage.

In the present paper, physical and methodical fundamentals of measuring the anomalous Nernst–Ettingshausen effect are considered via the example of CoPt ferromagnetic film structures. These alloys have already demonstrated their practical value for manufacturing sources and detectors of circularly polarized light [18] and as materials that realize low-dimensional magnetic configurations — skyrmions [19].

Basic relations between thermomagnetic and Hall coefficients, on the one hand, and parameters of the structures studied, on the other hand, are formulated. We present the result of experimental studies of the magnetic field dependences of Hall and Nernst–Ettingshausen voltages, and conclusions are made on the polarization of conductivity electrons participating in kinetic processes, as well as on the character of dominating mechanism of spin-dependent scattering and temperature dependence of the Fermi level position.

2. Theoretical description of anomalous thermomagnetic and galvanomagnetic phenomena

In this section, we consider one of the most common variants of thermomagnetic phenomena, the transverse Nernst–Ettingshausen effect (since we do not discuss the longitudinal effect here, we will simply call it the 'Nernst–Ettingshausen effect' below). This phenomenon is commonly considered in analogy with the Hall effect, namely, by the appearance of a difference in potentials transverse with respect to the current flowing through the sample in an external magnetic field. The cause of the effect is a trajectory deflection of free charge carriers under the action of the Lorentz force from the external magnetic field. In the presence of spin-dependent scattering of free charge carriers in a ferromagnetic structure, the anomalous component of the effect is added to the ordinary component, which distorts the linear magnetic field dependence of the effect [20]. The general expression for the Hall resistance R has the form

$$R = \frac{U_H}{I} = R_H H\mu_0 + R_{AH} M(H), \tag{1}$$

where R_H, R_{AH} are the ordinary and anomalous Hall constants, respectively, μ_0 is the magnetic constant, U_H is the transverse Hall voltage, I is the current flowing through the structure, H is the external magnetic field, and $M(H)$ is the magnetization of the structure depending on the external magnetic field.

In the case of the Hall effect, the driving force for transferring free charge carriers is the external electric field applied to the sample. The value of the ordinary Hall effect constant is determined by transport parameters, namely, the concentration and mobility of free charge carriers. The sign of the effect depends on the sign of the particles' charge.

The occurrence of an anomalous part in expression (1) leads to a distortion of the linear magnetic field dependence $R(H)$. The change in the character of the dependence is dictated by the magnetic field dependence of the structure magnetization $M(H)$ [20]. In contrast to the definition of the 'ordinary' constant, it is impossible to determine the 'anomalous' constant R_{AH} unambiguously from the Hall effect. From the form of the magnetic field dependence of the Hall resistance, it is possible to find the value of $R_{AH}M_s$, where M_s is the residual magnetization (in a zero magnetic field) at a given temperature. The value of the residual magnetization should be studied by other methods.

According to model considerations [21, 22], experimentally confirmed in Refs [23, 24], the value of the anomalous Hall constant in metals has a power dependence on the specific resistance of the structure,

$$R_{AH} = a\rho + b\rho^2, \tag{2}$$

where a and b are temperature-independent parameters, characterizing the metal's electronic structure. Numerical values of these parameters determine the dominant type of spin-dependent scattering of free charge carriers. So, at $a \gg b$, angular scattering dominates, for which the particle motion trajectory declines after interaction with a magnetic center. In the opposite case, side scattering is predominantly realized, which does not lead to a distortion of the particle trajectory [25].

The study of the magnetic field dependence of Hall resistance is a powerful informative technique for investigating the magnetic properties of materials; however, it is not fully self-sufficient. In contrast to the sign of R_H, the sign of the anomalous Hall coefficient does not depend on the type of free charge carrier. The sign of R_{AH} is determined by manifold factors, namely, the sign of charge carriers, mutual orientation of the current carrier spins, and the sample magnetiza-

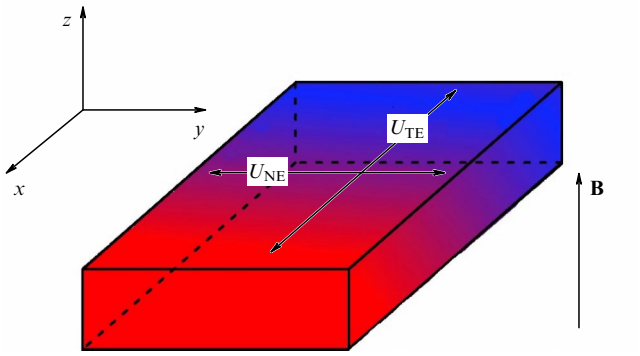

Figure 1. Schematic representation of setting up the problem of the occurrence of thermomagnetic and galvanomagnetic phenomena in a plane-parallel rectangular sample.

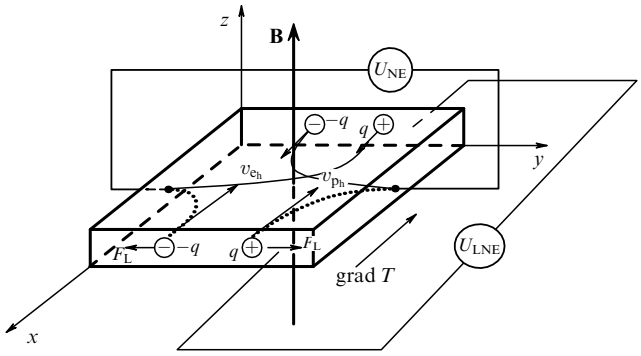

Figure 2. Schematic representation of the occurrence of the Nernst–Ettingshausen thermomagnetic effect.

tion vector. Moreover, the anomalous Hall effect measurements cannot unambiguously reveal the cause of magnetic ordering in the studied structure or allow only detecting the very fact of the presence of such ordering [20, 26]. Information on the magnetic properties of materials can be substantially completed by performing simultaneously a complex of thermoelectric and thermomagnetic studies.

Below, we present fundamental relations for describing thermomagnetic phenomena. Let us consider a plane-parallel sample (Fig. 1). When a temperature gradient $\operatorname{grad} T = \{\partial T/\partial x, 0, 0\}$ is created in the direction of the x-axis, a thermoelectric (Seebeck) effect arises in the structure due to the presence of a thermal flow of free charge carriers from the higher-temperature region to the lower-temperature one. This flow is compensated by the reverse flow in the electric field created by the excess concentration of carriers near the 'cold' face of the sample and the noncompensated ions near the 'hot' face [27]. As a result of the distribution of carriers between the hot and cold faces of the structure, an electric field arises,

$$\mathbf{E}_{TE} = \alpha \nabla T, \tag{3}$$

where ∇T is, in the general case, the temperature gradient between the hot and cold sample faces.

In the overwhelming majority of cases, a linear law of temperature variation in the direction of the x-axis is considered, so that the temperature gradient can be expressed as $\nabla T = \Delta T/d$, where d is the sample thickness, and ΔT is the temperature difference between the hot and cold ends. Hereinafter, in formulas for the thermal EMF, the difference ΔT rather than the temperature gradient is considered. The magnitude of thermal EMF U_{TE} as the work of thermal forces on moving the charges in the field $\mathbf{E}_{TE}$ is expressed as

$$U_{TE} = \alpha \Delta T. \tag{3'}$$

The Seebeck coefficient directly depends on the structure resistance: the higher the resistance, the greater the electric field necessary to compensate for the contrary heat flow. This dependence is determined by the relation of both quantities with the concentration of free charge carriers n. In the literature, the concentration dependence of the Seebeck coefficient and the specific resistance in semiconductor and metallic materials is presented in the following form [30]:

$$\alpha(n) = \frac{8\pi^2 k_B^2}{3eh^2}\, m^* T \left(\frac{\pi}{3n}\right)^{2/3}, \qquad \rho = \frac{1}{en\mu}, \tag{4}$$

where k_B is the Boltzmann constant, h is the Planck constant, m^* is the effective mass of free charge carriers, T is the mean temperature of the structure, e is the elementary charge, and μ is the mobility of free charge carriers.

In the metals considered here, the concentration of free charge carriers is high ($n > 10^{20} - 10^{22}$ cm^{-3}) and the value of the Seebeck coefficient does not exceed 5–20 μV K^{-1}, which does not allow obtaining voltages practically applicable for an autonomous supply. However, the Seebeck effect has a simple fundamental application for the determination of the type of free charge carrier (electrons or holes) by the sign of the arising thermal EMF [28].

If the structure is placed in an external magnetic field, then, in the direction of the vector product of the temperature gradient and the external magnetic field induction, a potential difference (Nernst–Ettingshausen voltage) U_{NE} arises (Fig. 2), in the general case expressed as [29]

$$Q = \frac{U_{NE}}{\Delta T} = Q_{NE} H \mu_0 + Q_{ANE} M(H), \tag{5}$$

where Q_{NE} is the ordinary Nernst–Ettingshausen constant, Q_{ANE} is the anomalous Nernst–Ettingshausen constant, and ΔT is the temperature difference between the faces of the structure. Here, Q [μV K^{-1}] is the transverse Nernst–Ettingshausen voltage normalized to the temperature gradient value, an analog of the Seebeck coefficient in the transverse direction of the temperature gradient.

The fundamental mechanism of the Nernst–Ettingshausen effect is similar in nature to the mechanism of the Hall EMF origin. As mentioned above, the temperature difference between the faces causes two counterpropagating fluxes of charge carriers. In an external magnetic field, the Lorentz force acts on these charge carriers, shifting their trajectory towards the samples faces. In a quasiequilibrium state, the current of carriers from the hot end of the sample to the cold one, caused by the temperature gradient, is compensated by the backward drift flow of carriers in the electric field, formed by the excess concentration of carriers at the cold end [30]. However, the velocities of the opposite currents are different due to the different nature of driving forces causing them. Therefore, the force acting on the thermal current differs in absolute value from the one acting on the current of charge carriers in an electric field, and is directed oppositely. This leads to an inhomogeneous distribution of carriers in the direction perpendicular to the heat flux and magnetic field (see Fig. 2) and, consequently, to the appearance of an electric field (voltage) in this direction. The considered process is

described by the 'ordinary' constant of the Nernst–Ettingshausen effect Q_{NE} in Eqn (5). The magnitude of the effect is determined by the temperature dependence of scattering (i.e., resistance). In metals and highly doped semiconductors, the Nernst–Ettingshausen voltage does not exceed 1–30 μV, which also limits practical applications of the effect [31, 32].

The main difference between 'ordinary' Hall and Nernst–Ettingshausen effects is that, in the case of the thermomagnetic effect, the direction of the heat flux does not depend on the kind of charge carrier. Therefore, the sign of the Nernst–Ettingshausen EMF is also independent of the kind of charge carrier and is determined by the character of carrier scattering. For example, when scattering by impurity centers dominates, the thermal flow of carriers will scatter more weakly than the flow caused by the action of electric forces. When scattering by phonons dominates, the situation is the opposite. It is interesting that, in the case of a superposition of two scattering mechanisms, a situation can take place in which no ordinary Nernst–Ettingshausen effect will appear, since the flows of charge carriers in the direction perpendicular to the temperature gradient will compensate each other.

Coefficient Q_{ANE} describes the anomalous Nernst–Ettingshausen effect in Eqn (5) due to the spin-dependent character of scattering in ferromagnetics. As is known, in ferromagnets, the scattering of charge carriers by a magnetic center depends on the mutual orientation of their spins. In the presence of an increased concentration of carriers with one spin value, this additionally contributes to the Hall and Nernst–Ettingshausen EMF [33, 34]. In contrast to the 'ordinary' Nernst–Ettingshausen effect, whose magnitude is determined by the temperature dependence of scattering, the magnitude of the anomalous effect is determined by the temperature dependence of spin scattering of carriers, characterized by the parameter of spin diffusion length. This parameter in ferromagnetic metals depends on temperature, as shown in a series of papers [35–37].

Based on the theoretical models developed in Refs [21, 22], by analogy with the anomalous Hall effect for metals, we can write

$$Q_{ANE} = -(\alpha + \beta\rho)T, \tag{6}$$

where α and β are temperature-independent coefficients characterizing the metal's electronic structure [38, 39]. Relation (6) has been experimentally confirmed for a number of ferromagnetic alloys [40].

Neither the sign nor the magnitude of the anomalous Nernst–Ettingshausen effect itself allows unambiguous conclusions on the causes and mechanisms of magnetic ordering in a studied object. However, simultaneous investigations of the anomalous Hall effect and the anomalous Nernst–Ettingshausen effect is a powerful tool to study the magnetism that allows overcoming the difficulties inherent in each of the methods separately. For example, by analogy with the anomalous Hall effect, it is impossible to separate the anomalous coefficient Q_{ANE} from the experimentally obtained magnetic field dependence of the Nernst–Ettingshausen voltage, since the particular form of the magnetic field dependence of the structure magnetization $M(H)$ is, generally, unknown. As in the Hall effect, the anomalous part of the magnetic field dependence of the Nernst–Ettingshausen voltage repeats the form of the dependence of the sample magnetization on the external magnetic field strength. From the data from experiments on the study of the magnetic field dependence of the thermomagnetic effect, it is possible to calculate the product $Q_{ANE}M_s$.

However, having simultaneously the data on the signs of the anomalous Hall and Nernst–Ettingshausen constants, it is possible to reach a conclusion about the type of free charge carriers participating in kinetic phenomena and their spin orientation [41]. In the case of $Q_{ANE} > 0$, the average magnetic moment of the carriers responsible for the kinetic phenomena in a ferromagnet is directed opposite to the resulting magnetization of the sample, a positive value of R_{AH} indicates that such carriers are holes, and, if $R_{AH} < 0$, they are electrons. When $Q_{ANE} < 0$, the mean magnetic moment of the carriers is codirected with the magnetization of the structure, and to determine the sign of the carriers with respect to the sign of the anomalous Hall constant, the situation is vice versa.

It is also known that, for $Q_{ANE} > 0$, $\alpha < 0$, $\beta < 0$, the spontaneous magnetization in the material is due to localized d-electrons, while at $Q_{ANE} < 0$, $\alpha > 0$, $\beta > 0$, the conductivity electrons contribute to the spontaneous magnetization [21, 22, 41]. Thus, the estimation of the above parameters gives information on the magnetic ordering mechanism in the object under study.

According to Ref. [21], the anomalous Hall and Nernst–Ettingshausen coefficients are related as

$$\frac{Q_{ANE}\rho}{R_{AH}} = \frac{\pi^2 k_B^2 T}{3e\langle\varepsilon_n\rangle}, \tag{7}$$

where $\langle\varepsilon_n\rangle = \langle E_F - E_{0n}\rangle$ is the total chemical potential value averaged over all conduction bands, E_F is the Fermi level position, and E_{0n} is the electron energy near the edge of the nth band.

The study of the temperature dependence of the ratio of anomalous Hall and Nernst–Ettingshausen coefficients will allow analyzing the dynamics of the relative position of the averaged energy level of conduction electrons and the Fermi level position. From Eqn (7), it is seen that, upon a decrease in $\langle\varepsilon_n\rangle$, the anomalous component of the Nernst–Ettingshausen effect increases. By controlling the parameter $\langle\varepsilon_n\rangle$, it is possible to substantially increase the anomalous component of the thermomagnetic effect, the ordinary components determined by transport parameters being small. Such a situation can occur in metallic and semiconductor films with a complex magnetic structure. Thus, in [42], a strong thermomagnetic effect is demonstrated in a Co_2MnGa film. The effect in Fe_3GeTe_2 and Mn_3X films (where X = Sn, Ge, Ga) has been shown in Refs [43, 44], respectively.

3. Thin metal CoPt films

In view of the foregoing, there is fundamental interest in the study of the thermomagnetic and galvanomagnetic properties of semiconductor and thin metallic films with a complex structure and composition. Of interest are magnetic alloys with an easy magnetization axis perpendicular to the film surface, since, for the practical realization of thermomagnetic phenomena in such alloys, it is necessary to create a longitudinal temperature gradient, which is simple to implement technically. Such systems include films of the CoPt system, possessing a perpendicular magnetic anisotropy [18, 45] and residual magnetization, close in magnitude to the saturation magnetization. Magnetization reversal fields of $\sim 50-1000$ Oe for the above structures can be

obtained without using superconducting magnets. Practically, the CoPt alloy is used in a spin light emitting diode (a source of circularly polarized radiation) as the material injecting spin-polarized free charge carriers into the semiconductor. The authors of Ref. [46] show the possibility of changing the magnetic properties of CoPt in a wide range by implanting He^+ ions. A detailed analysis of the magnetic domain structure in CoPt films is presented in Ref. [47].

In the present paper, a CoPt film formed on a substrate of semi-insulating gallium arsenide of (100) orientation is used as a subject of study. In a number of papers [48, 49], it is pointed out that the main method of fabricating CoPt films is magnetron sputtering on an MgO substrate with various orientations. In analogy with Ref. [18], our structures were films of the $Co_{45}Pt_{55}$ alloy obtained by the electron beam evaporation method at a temperature of 200 °C. The films were formed on i-GaAs (001) substrates over the previously deposited thin ($\sim$ 1 nm) layer of Al_2O_3 by alternating the deposition of Pt (0.5 nm) and Co (0.3 nm) layers. The previously formed thin layer of aluminum oxide is necessary to prevent the diffusion of Co atoms into the GaAs substrate [45, 50]. The total CoPt film thickness is $\sim$ 8 nm.

In the studied film, due to the low mobility of free charge carriers, the ordinary components of the above effects are small ($R_H \ll R_{AH}$ and $Q_{NE} \ll Q_{ANE}$), which allows simplifying Eqns (1) and (5), namely, eliminating the terms that describe the contribution from ordinary effects:

$$Q = Q_{ANE} M\,, \qquad R = R_{AH} M\,. \tag{8}$$

The smallness of ordinary components in Eqns (1) and (5) is experimentally confirmed below.

4. Experimental technique

To study the magnetic properties of the structures, we recorded the magnetic field dependence of Hall and Nernst–Ettingshausen voltages.

A schematic diagram showing the fixing of the structure is shown in Fig. 3a. The top face of the sample is conventionally divided into a proportion of 1:2. A resistor heater is installed on the smaller part. The value of the current passed through the resistor determines the temperature of the structure. The face opposite face *2* is pressed towards the massive metallic radiator *6*, by means of which the heat flux is drained from the 'cold' face of the sample and the temperature gradient is set.

Figures 3b–d illustrate the soldering of the sample with six ohmic contacts of indium formed on the structure surface. The contacts serve to measure the specific resistance (Fig. 3b), Hall resistance (Fig. 3c), and Nernst–Ettingshausen coefficient (Fig. 3d). Unidirectional arrows show the directions of current flow; bidirectional ones show the recorded voltage.

The specific resistance is recorded using a standard Van der Pauw four-point probe circuit. The techniques for recording the Hall effect are well known and presented in a vast number of publications (see, e.g., [51, 52]). To record the magnetic field dependence of the Nernst–Ettingshausen voltage, electric current was passed through the resistor (GH), heating one side of the structure. Because of the heat drain by the radiator, a temperature gradient was created in the structure volume. The voltage arising in the magnetic field was recorded at the contacts (CD). The magnetic field was directed perpendicular to the film surface. Additionally, the

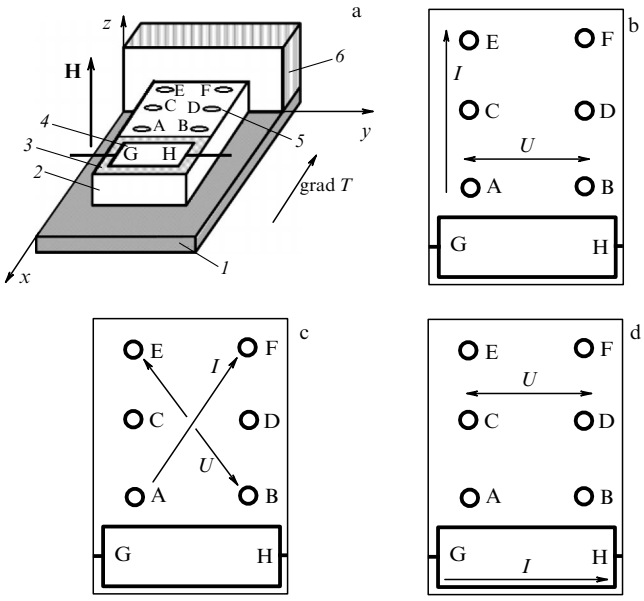

Figure 3. (a) Schematic view of fixing a sample on a six-contact holder to record the Hall and Nernst–Ettingshausen effects: *1* — holder, *2* — sample, *3* — mica, *4* — resistor heater, *5* — contact, *6* — radiator. (b) Schematic diagram of measuring the resistance. (c) Schematic diagram of measuring the Hall effect. (d) Schematic diagram of measuring the Nernst–Ettingshausen effect.

Nernst–Ettingshausen voltage recording technique used by us can be found in [53–55].

The sample was placed in a helium closed-cycle Janis CCS-300S/202 cryostat, allowing measurements in a wide range of temperatures (10–400 K). A temperature sensor based on a silicon diode was built in the cryostat to record the temperature of the metallic rod, on which the sample holder was fixed. The heat drain from the sample through the radiator occurred directly into the rod, which allowed considering the temperature of the cold face approximately equal to that of the metallic rod. The sample hot face temperature was evaluated from the resistance of the heater resistor with the known calibration characteristic. To heat the resistor, a Keithley 6221 measuring current source was used, which allowed setting the current with an accuracy of up to 2 nA. To stabilize the temperature gradient, a LakeShore 335 temperature controller with a PID-system (proportional-plus-integral-plus-derivative (PID) controller) was used. The controller fixed the temperature of the sample cold face, while the temperature of the hot face and the value of the temperature gradient were specified by choosing the current through the resistor. In the experiment, the current was chosen such that the temperature gradient was 10 K with an accuracy of up to 0.1 K. To ensure such an accuracy, the system was let alone a long time to establish quasi-thermodynamic equilibrium, the time interval being as long as an hour. The Nernst–Ettingshausen and Hall voltages were measured using an automated Kethley-2400 voltmeter. The magnitude of magnetic field induction was recorded by means of a magnetic field sensor based on the indium antimonide using an automated L-CARD E14-140MD data acquisition system. Due to the complex study of magnetic field dependences of Hall and Nernst–Ettingshausen voltages under cryogenic temperature conditions, it is possible to study the parameters of electron transport in thin metallic films ferromagnetic systems.

5. Experimental results

In the experiment, the magnetic field dependences of Hall and Nernst–Ettingshausen voltages were recorded, as was the specific resistance within a temperature interval of 10–362 K.

Figure 4 shows the temperature dependence of the specific resistance of the structure. With decreasing temperature, the resistance of the structure decreases, thus confirming the metallic character of the conductivity in the sample.

The magnetic field dependences of the Hall resistance at some temperatures are shown in Fig. 5a. The experimental curves have the shape of a hysteresis loop, which indicates the presence of ferromagnetic ordering in the studied metal layer. The obtained results are in good agreement with the data of Ref. [18]. It is important to note that, at a magnetic field magnitude exceeding the coercive field H_c, the Hall resistance does not change until the moment of structure magnetization reversal ($H = -H_c$). Therefore, the ordinary Hall effect is small compared to the contribution of the anomalous component in Eqn (1), so that the simplified expression (8) can be used for the analysis. The value of H_c increases with a decrease in temperature. The hysteresis loop width is determined by specific features of the domain structure of the studied system, discussed in detail in Ref. [47].

The magnetic field dependence of the normalized Nernst–Ettingshausen voltage repeats the magnetic field dependence of the Hall resistance in the entire temperature interval studied (Fig. 5b). Due to the presence of strong thermal noises, we could not detect the Nernst–Ettingshausen effect at temperatures below 125 K. However, the anomalous Hall effect has been observed at temperatures up to 10 K. The loop width in the Nernst–Ettingshausen effect, as in the Hall effect, is determined by the domain structure and, therefore, the values of coercive fields should be comparable for both effects [56]. Such a comparison is demonstrated in Fig. 6, where the magnetic field dependences of both effects at the average temperature of 250 K of the sample are shown. The Nernst–Ettingshausen voltage is seen to depend on the structure magnetization state; therefore, due to the residual magnetization of the film upon switching off the external magnetic field, the transverse voltage is practically unchanged. The values of thermomagnetic voltage obtained by us are comparable to the data published earlier (see, e.g., [42–44]). It is remarkable that the magnetized system 'remembers' its state, the temperature gradient being a 'power supply' for such a 'memory cell.' To 'record' an opposite bit of information, it is necessary to reverse either the film magnetization or the temperature gradient. The anomalous Nernst–Ettingshausen effect manifests itself over the entire temperature measurement range, becoming even stronger with an increase in temperature. However, with growing temperature, the value of the magnetization reversal field decreases, which makes such a memory cell somewhat less stable.

It is important to note that, because of the asymmetric position of contacts C and D (see Fig. 3) with respect to the temperature gradient direction, an error may appear in the measured value of the Nernst–Ettingshausen voltage due to the additive contribution of the thermoelectric Seebeck effect. This leads to a shift of the curve along the y-axis, which can be an odd function of the magnetic contribution (due to the longitudinal Nernst–Ettingshausen effect) rather than a constant. To estimate the influence of the thermoelectric effect on the value of Nernst–Ettingshausen voltage, we

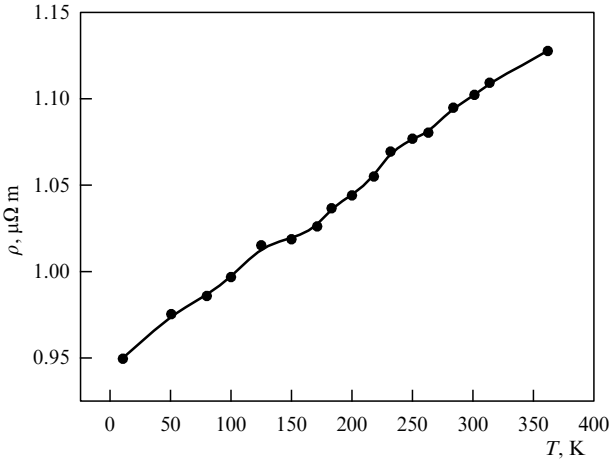

Figure 4. Experimentally obtained temperature dependence of the specific resistance of the studied structure.

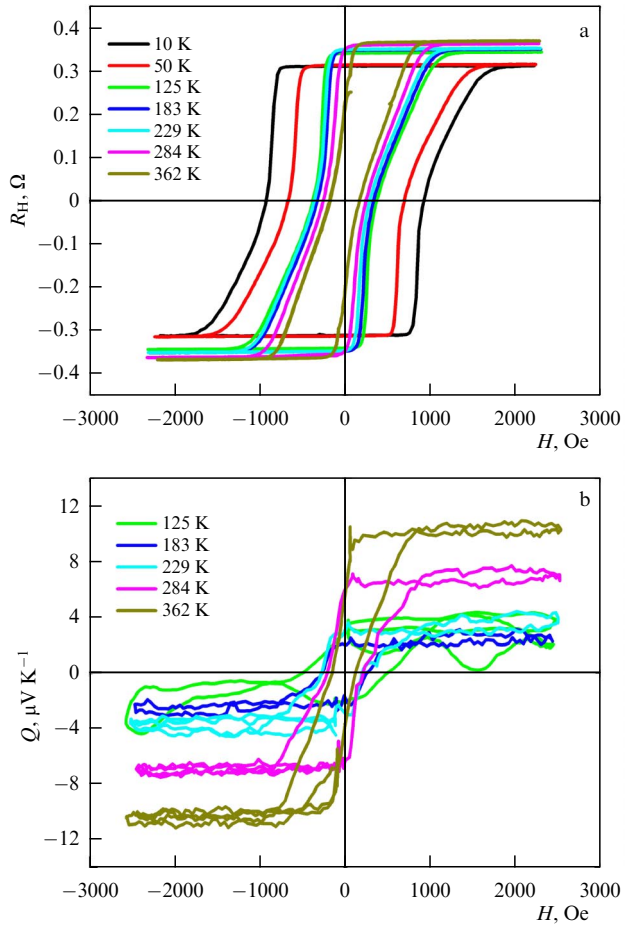

Figure 5. Experimentally obtained magnetic field dependences of (a) the Hall resistance, (b) the Nernst–Ettingshausen voltage normalized to the value of the temperature gradient in the temperature interval of 10–362 K.

recorded the thermal EMF between the contacts AE and BF, which appeared to be less than 1 μV K^{-1} and weakly dependent on the magnetic field in the range of experimentally measured field values. Since, at contacts C and D, the temperature gradient is extremely small because of their close spacing with respect to the temperature gradient propagation, the thermal EMF signal is significantly weaker than the Nernst–Ettingshausen voltage.

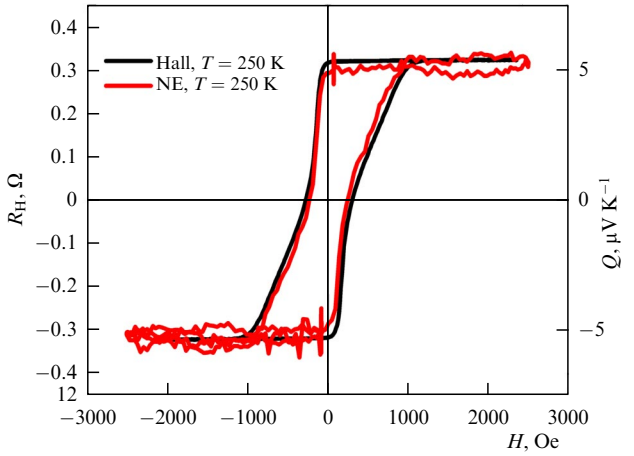

Figure 6. Comparison of experimentally obtained magnetic field dependences of the Hall resistance and Nernst–Ettingshausen voltage normalized to the temperature gradient, recorded at an average temperature of 250 K of the structure.

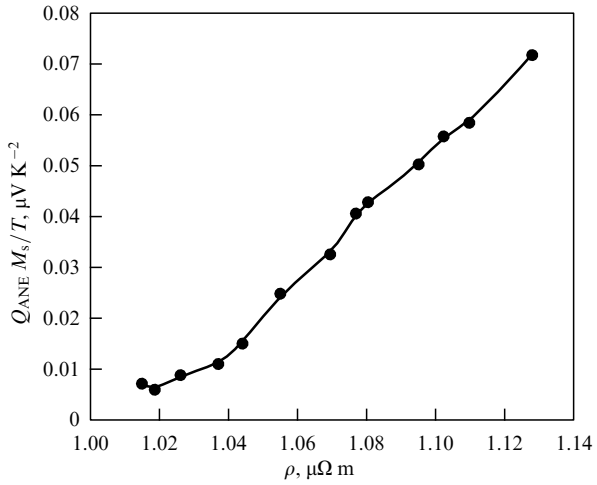

Figure 8. Experimentally obtained dependence of $Q_{ANE}M_s/T$ on the specific resistance.

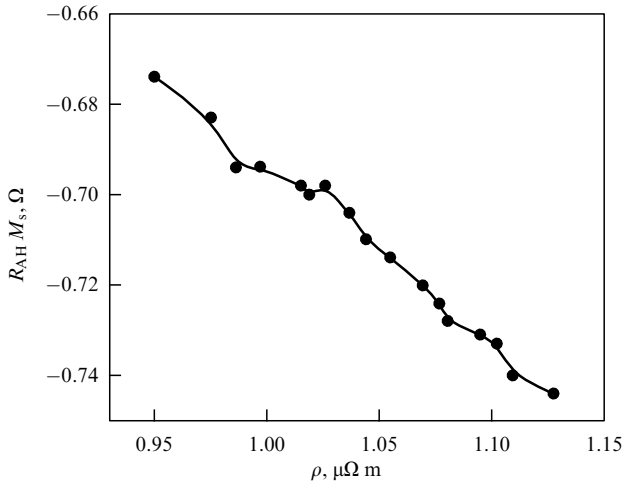

Figure 7. Experimentally obtained dependence of $R_{AH}M_s$ on the specific resistance.

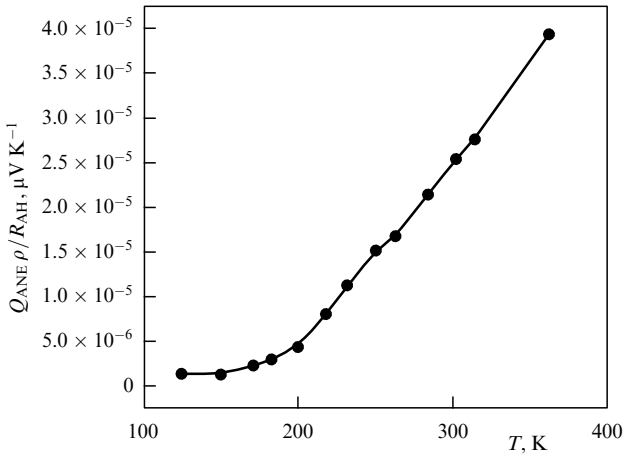

Figure 9. Experimentally obtained temperature dependence of the quantity $Q_{ANE}\rho/R_{AH}$.

As was mentioned above, besides the possibility of practical application considered in the literature, the thermomagnetic Nernst–Ettingshausen effect is a powerful tool for studying magnetic properties. Figure 7 shows the dependence of $R_{AH}M_s$ on the specific resistance. The dependence is seen to have a linear character, which indicates the dominance in the transport of angular spin-dependent scattering, at which the free charge carrier trajectory is deflected because of interaction with a magnetic center. The anomalous Hall constant is negative in the entire interval of temperatures. From the dependence slope, it is seen that the coefficient a is less than zero.

The residual magnetization measured at room temperature by the variable field gradient method [57] amounted to 70 G. From the experimental curves of magnetic field dependences of Hall and Nernst–Ettingshausen coefficients, it is possible to find the products $R_{AH}M_s$ and $Q_{ANE}M_s$, which is sufficient information for analyzing the temperature curves, as well as the dependences of these values on the values of specific resistance of the film at a fixed temperature. In other words, there is no need to obtain absolute values of the magnetization in the entire temperature interval measured.

Figure 8 presents the dependence of $Q_{ANE}M_s/T$ on the specific resistance, from which it is seen, in accordance with (6), that $Q_{ANE} > 0$ and $\beta < 0$.

Thus, the analysis of experimental values of thermomagnetic coefficients revealed that $Q_{ANE} > 0$, $R_{AH} < 0$, $\alpha < 0$, and $\beta < 0$, from which a conclusion follows that the main free charge carriers participating in kinetic phenomena are electrons, whose average magnetic moment is directed against the resulting magnetization of the sample. An additional method for analyzing the sign of the carriers is to record the thermal EMF. In the entire range of measured temperatures, the longitudinal Seebeck voltage had a negative sign. The localized d-shell electrons introduce the dominant contribution to the presence of spontaneous magnetization. In addition, it is important to note that the experimental dependences are well described by expressions (2) and (6), thus confirming the validity of applying the above theory to CoPt alloys.

Figure 9 presents the experimental temperature dependence of the quantity $Q_{ANE}\rho/R_{AH}$. The dependence is seen to be nonlinear at temperatures below 200 K, which is explained by the temperature dependence of the Fermi level

position $\langle \varepsilon_n \rangle(T)$. However, in the temperature range $362 > T > 200$ K, the dependence becomes linear, indicating the weakness of the temperature dependence of $\langle \varepsilon_n \rangle$ in this range. From Eqn (7), it is seen that, the smaller $\langle \varepsilon_n \rangle$, the higher the ratio of anomalous coefficients. In the present case, the position of the Fermi level is unchanged upon the temperature reaching 200 K; therefore, the growth of the thermomagnetic effect magnitude is due only to an increase in the specific resistance of the structure. As was shown above, the $Co_{45}Pt_{55}$ alloy demonstrates high thermomagnetic performance; therefore, it is assumed that, by varying the alloy composition, it would be possible to control the values of $\langle \varepsilon_n \rangle$ with the purpose of achieving the maximum efficiency of the thermomagnetic phenomenon expression.

6. Conclusion

'Ordinary' and anomalous transverse Nernst–Ettingshausen effects are considered. The fundamentals of theoretical models for galvanomagnetic and thermomagnetic effects are presented. Wide experimental potentialities are shown for the complex investigation of galvanomagnetic and thermomagnetic phenomena in order to study the electronic structure and electronic and magnetic properties of thin film semiconductor and metallic structures.

For a sample of a $Co_{55}Pt_{45}$ alloy thin film, the thermomagnetic effect characteristics were measured and calculated. The effect parameters were analyzed, and conclusions were made about the specific features of magnetic ordering and magnetotransport mechanisms. For example, based on the obtained experimental curves, it is concluded that electrons are the main charge carriers participating in kinetic phenomena in $Co_{45}Pt_{55}$ alloy layers. As follows from analyses of the temperature dependences of the anomalous Hall and Nernst–Ettingshausen effects, the main contribution to a film's spontaneous magnetization comes from the localized d-shell electrons, and the angular spin-dependent mechanism of free charge carrier scattering dominates.

Results concerning taking into account the Nernst–Ettingshausen effect in thin ferromagnetic films are a perfect demonstration of applying thermal spintronics, which offers one more degree of freedom in the development of electronic devices using the spins of free charge carriers.

The study was supported by the Russian Science Foundation (grant no. 21-79-20186, Fabrication of CoPt Films) and the Russian Foundation for Basic Research (grant no. 20-38-70063, Performing Galvanomagnetic and Thermomagnetic Studies).

References

1. Alisultanov Z Z *JETP Lett*. **99** 702 (2014); *Pis'ma Zh. Eksp. Teor. Fiz*. **99** 813 (2014)
2. Kolomoets N V, Laptev S A, Rogacheva E I *Sov. Phys. Semicond.* **20** 283 (1986); *Fiz. Tekh. Poluprovodn.* **20** 447 (1986)
3. Zhitinskaya M K, Nemov S A, Ivanova L D *Phys. Solid State* **44** 42 (2002); *Fiz. Tverd. Tela* **44** 41 (2002)
4. Wu H et al. *J. Magn. Magn. Mater*. **441** 149 (2017)
5. Park G-H et al. *Phys. Rev. B* **101** 060406 (2020)
6. Kuznetsov Y et al. *J. Phys. Conf. Ser*. **1695** 012145 (2020)
7. Ramos R et al. *Phys. Rev. B* **90** 054422 (2014)
8. Xu J, Phelan W A, Chien C-L *Nano Lett*. **19** 8250 (2019)
9. Ranjbar B, Mehrpooya M, Marefati M *Renewable Energy* **164** 194 (2021)
10. Ren W et al. *Sci. Adv*. **7** eabe0586 (2021)
11. Kuznetsov Yu et al. *AIP Adv*. **10** 065219 (2020)
12. Sakuraba Y *Scr. Mater*. **111** 29 (2016)
13. Mizuguchi M, Nakatsuji S *Sci. Technol. Adv. Mater*. **20** (1) 262 (2019)
14. Ikhlas M et al. *Nat. Phys*. **13** 1085 (2017)
15. Cohn J L et al. *Phys. Rev. Lett*. **108** 056604 (2012)
16. Mizuguchi M et al. *Appl. Phys. Express* **5** 093002 (2012)
17. Sakuraba Y et al. *Appl. Phys. Express* **6** 033003 (2013)
18. Zdoroveyshchev A V et al. *Semiconductors* **49** 1601 (2015); *Fiz. Tekh. Poluprovodn*. **49** 1649 (2015)
19. Sapozhnikov M V et al. *JETP Lett*. **107** 364 (2018); *Pis'ma Zh. Eksp. Teor. Fiz*. **107** 378 (2018)
20. Nagaosa N et al. *Rev. Mod. Phys*. **82** 1539 (2010)
21. Kondorskii E I *Sov. Phys. JETP* **19** 1406 (1964); *Zh. Eksp. Teor. Fiz*. **46** 2085 (1964)
22. Kondorskii E I, Cheremushkina A V, Kurbaniyazov N *Phys. Solid State* **6** 422 (1964); *Fiz. Tverd. Tela* **6** 539 (1964)
23. Chernoglazov K Yu et al. *JETP Lett*. **103** 476 (2016); *Pis'ma Zh. Eksp. Teor. Fiz*. **103** 539 (2016)
24. Nikolaev S N et al. *JETP Lett*. **89** 603 (2009); *Pis'ma Zh. Eksp. Teor. Fiz*. **89** 707 (2009)
25. Taylor G R, Isin A, Coleman R V *Phys. Rev*. **165** 621 (1968)
26. Kudrin A V et al. *Phys. Rev. B* **90** 024415 (2014)
27. Nadtochiy A et al. *Sci. Rep*. **9** 16335 (2019)
28. Shalimova K V *Fizika Poluprovodnikov* (Physics of Semiconductors) (St. Petersburg: Lan', 2010)
29. Arsen'eva A D et al. *Fiz. Tverd. Tela* **335** 1443 (1991)
30. Tsidil'kovskii I M *Thermomagnetic Effects in Semiconductors* (London: Infosearch, 1962); Translated from Russian: *Termomagnitnye Yavleniya v Poluprovodnikakh* (Moscow: GIFML, 1960)
31. Behnia K, Aubin H *Rep. Prog. Phys*. **79** 046502 (2016)
32. Kuznetsov Yu M et al. *J. Phys. Conf. Ser*. **933** 012015 (2018)
33. Aronzon B A et al. *Phys. Solid State* **49** 171 (2007); *Fiz. Tverd. Tela* **49** (1) 165 (2007)
34. Kusraev Yu G *Phys. Usp*. **53** 725 (2010); *Usp. Fiz. Nauk* **180** 759 (2010)
35. Isasa M et al. *Phys. Rev. B* **91** 024402 (2015)
36. Sasaki T et al. *Appl. Phys. Lett*. **96** 122101 (2010)
37. Yakata S et al. *Jpn. J. Appl. Phys*. **45** 3892 (2006)
38. Kondorskii E I *Sov. Phys. JETP* **21** 337 (1965); *Zh. Eksp. Teor. Fiz*. **48** 506 (1965)
39. Berger L *Phys. Rev. B* **5** 1862 (1972)
40. Kondorskii E I et al. *JETP Lett*. **10** 49 (1969); *Pis'ma Zh. Eksp. Teor. Fiz*. **10** 78 (1969)
41. Kondorskii E I *Sov. Phys. JETP* **28** 291 (1969); *Zh. Eksp. Teor. Fiz*. **55** 558 (1968)
42. Reichlova H et al. *Appl. Phys. Lett*. **113** 212405 (2018)
43. Xu J, Phelan W A, Chien C-L *Nano Lett*. **19** 8250 (2019)
44. Guo G-Y, Wang T-C *Phys. Rev. B* **96** 224415 (2017)
45. Zdoroveyshchev A V et al. *Phys. Solid State* **58** 2267 (2016); *Fiz. Tverd. Tela* **58** 2186 (2016)
46. Kalentyeva I L et al. *Phys. Solid State* **63** 386 (2021); *Fiz. Tverd. Tela* **63** 324 (2021)
47. Temiryazev A G et al. *Phys. Solid State* **60** 2200 (2018); *Fiz. Tverd. Tela* **60** 2158 (2018)
48. Sato H et al. *J. Appl. Phys*. **103** 07E114 (2008)
49. Kim P D et al. *Tech. Phys*. **49** 431 (2004); *Zh. Tekh. Fiz*. **74** (4) 53 (2004)
50. Kudrin A V et al. *Phys. Solid State* **59** 2220 (2017); *Fiz. Tverd. Tela* **59** 2203 (2017)
51. Sinova J, MacDonald A H, in *Semiconductors and Semimetals* Vol. 82 (Ed. E R Weber) (Amsterdam: Elsevier, 2008) p. 45
52. Nagaosa N et al. *Rev. Mod. Phys*. **82** 1539 (2010)
53. Kuznetsov Yu M et al. *J. Phys. Conf. Ser*. **933** 012015 (2018)
54. Kuznetsov Y et al. *J. Phys. Conf. Ser*. **1124** 061004 (2018)
55. Kuznetsov Y et al. *J. Phys. Conf. Ser*. **1695** 012145 (2020)
56. Arsenieva A D et al. *J. Magn. Magn. Mater*. **99** 167 (1991)
57. Flanders P J *J. Appl. Phys*. **63** 3940 (1988)